

# Shape from Semantics: 3D Shape Generation from Multi-View Semantics

LIANGCHEN LI, University of Science and Technology of China, China  
 CAOLIWEN WANG, University of Science and Technology of China, China  
 YUQI ZHOU, University of Science and Technology of China, China  
 BAILIN DENG, Cardiff University, United Kingdom  
 JUYONG ZHANG\*, University of Science and Technology of China, China

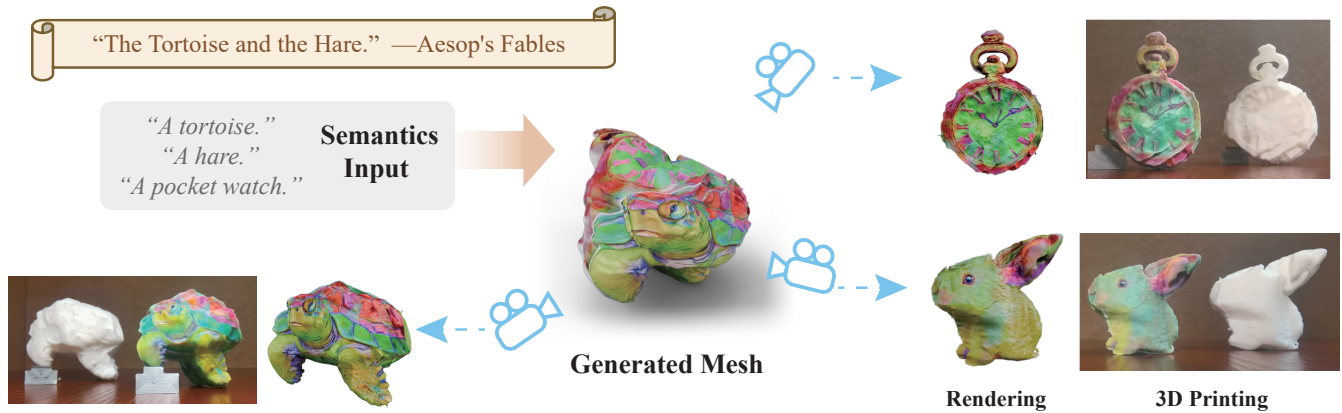


Fig. 1. We propose and address **Shape from Semantics**, a novel generative problem. Given a set of semantics and corresponding views as input, our method can produce high-quality shapes that exhibit geometry and appearance consistent with the semantics from each view and are feasible for real-world fabrication.

We propose “Shape from Semantics”, which is able to create 3D models whose geometry and appearance match given semantics when observed from different views. Traditional “Shape from X” tasks usually use visual input (e.g., RGB images or depth maps) to reconstruct geometry, imposing strict constraints that limit creative explorations. As applications, works like Shadow Art and Wire Art often struggle to grasp the embedded semantics of their design through direct observation and rely heavily on specific setups for proper display. To address these limitations, our framework uses semantics as input, greatly expanding the design space to create objects that integrate multiple semantic elements and are easily discernible by observers. Considering that this task requires a rich imagination, we adopt various generative models and structure-to-detail pipelines. Specifically, we adopt multi-semantics Score Distillation Sampling (SDS) to distill 3D geometry and appearance from 2D diffusion models, ensuring that the initial shape is consistent with the semantic input. We then use image restoration and video generation models to add more details as supervision. Finally, we introduce neural signed distance field (SDF) representation to achieve detailed shape reconstruction. Our framework generates meshes with complex details, well-structured geometry, coherent textures, and smooth transitions, resulting in visually appealing and eye-catching designs. Project page: <https://shapefromsemantics.github.io>.

CCS Concepts: • **Computing methodologies** → **Shape modeling**; *Rendering*; *Machine learning approaches*.

\*Corresponding author (juyong@ustc.edu.cn).

Authors’ Contact Information: Liangchen Li, liangchen@mail.ustc.edu.cn, University of Science and Technology of China, China; Caoliwen Wang, wclw1021@mail.ustc.edu.cn, University of Science and Technology of China, China; Yuqi Zhou, sasuke18@mail.ustc.edu.cn, University of Science and Technology of China, China; Bailin Deng, DengB3@cardiff.ac.uk, Cardiff University, United Kingdom; Juyong Zhang, juyong@ustc.edu.cn, University of Science and Technology of China, China.

Additional Key Words and Phrases: inverse modeling, generative priors

## 1 Introduction

Reconstructing 3D geometry from given information is a fundamental problem in computer graphics and computer vision, with broad applications in areas such as cultural heritage digitization, film, and architecture. Conventional “Shape from X” methods typically rely on specific visual data such as RGB images, depth maps or surface normals to reconstruct 3D geometry and renderings that closely match the target. However, while these inputs provide sufficient information for accurate reconstruction, they introduce strict constraints that hinder the generation of imaginative and novel 3D assets, which are critical for applications in AR/VR and art.

To address these limitations, we propose a novel “Shape from Semantics” problem that utilizes textual descriptions, or semantics, to guide the generation of 3D geometry. In this context, semantics refer to high-level, human-interpretable concepts or attributes that describe the desired appearance or characteristics of an object. By using semantics as input, our approach enables creating 3D models that convey the intended visual properties from multiple viewpoints, introducing a new level of flexibility and creativity to the “Shape from X” reconstruction paradigm. Unlike traditional methods that aim to reconstruct a specific object based on captured visual data, our approach allows users to generate 3D models that match a broader set of desired attributes described by the input semantics. This expands the design space and empowers users to create imaginative and compelling 3D objects that align with their creative intent. The resulting 3D models can be directly observed from different views,

providing a more intuitive and immersive experience compared to 2D designs or projections. Moreover, semantics-based operations are inherently more user-friendly, allowing users to generate intricate textures and detailed meshes with just a few text prompts. This significantly lowers the barrier to artistic creation, enabling non-professionals to produce stunning works of art.

Our proposed problem is non-trivial because we aim to match the shape geometry and appearance from different viewpoints with input semantics rather than specific input images, making existing multi-view reconstruction approaches inapplicable. Moreover, current text-to-3D generation models are not suitable either, as they typically use a single prompt to describe a single object, while our approach uses multiple input prompts that describe different objects for the appearance of the shape in different view directions. The most similar current research to ours explores utilizing information such as shadows and contours as the basis for reconstruction and design. For instance, Shadow Art [Mitra and Pauly 2009] aims to create objects whose projections under specific lighting conditions match the given constraints. Wire Art [Hsiao et al. 2018; Qu et al. 2024; Tojo et al. 2024] focuses on generating wireframe geometries that align with the input 2D line drawings or that can outline shapes consistent with the provided semantic inputs. However, the visual experience provided by these designs is primarily two-dimensional. When directly observing the objects, it is often challenging to perceive the embedded semantic information that the designs aim to convey. Furthermore, these techniques often rely on specific setups, such as light sources and projection planes, while also facing challenges in fabrication, which limits their practical applications.

To solve the novel problem proposed above, our key idea is to utilize the image- and text-understanding capabilities of generative models to create a 3D shape that matches the input semantics when observed from different directions. Our structure-to-detail approach is divided into three stages. In the first stage, we utilize a semantic-guided diffusion model prior [Poole et al. 2022; Tang et al. 2023a] to construct coarse geometry and texture represented as 3D Gaussian Splatting (3DGS) [Kerbl et al. 2023]. We employ multi-semantics Score Distillation Sampling (SDS) to distill 3D geometry and appearance from 2D diffusion models, ensuring that the initial shape aligns with the semantic input. In the second stage, we refine the generated textures using an image diffusion model [Yu et al. 2024b]. At the same time, we employ a video diffusion model [Sun et al. 2024] to estimate rendering results from various satellite views, which provide priors for training neural implicit representations in the subsequent stage. This multi-view approach helps ensure that the model’s geometry is consistent and perceptually coherent from different views. Finally, in the third stage, we represent the refined 3D model using neural implicit representations of Signed Distance Functions (SDF) [Park et al. 2019; Wang et al. 2021]. The training of this SDF model is guided by the coarse 3DGS geometry masks and the detailed texture maps derived from satellite views. This process enables the neural implicit representation to capture both the final shape and texture of the object. From this representation, we extract a fabricable high-quality mesh, which preserves the geometry, textures, and smooth transitions required for practical use.

Our results demonstrate that specific viewpoints of the same object effectively integrate multiple semantic elements, which are

easily discernible to observers. The models produced by our method exhibit a high degree of creativity, often surpassing what can be achieved through traditional spatial intuition or non-semantic inputs. The final high-quality meshes feature intricate details, well-constructed geometry, cohesive textures, and smooth transitions, resulting in visually engaging and compelling designs. Moreover, these models are manufacturable, significantly enhancing their practical applicability and expanding their potential for real-world use. In summary, our contributions include:

- We introduce the “Shape from Semantics” problem, where semantic input guides the generation and design of 3D models with perceptual 3D characteristics. Unlike traditional “Shape from X” approaches, our focus is on creating highly imaginative and visually compelling geometric objects.
- We employ a range of generative models to address this problem, bridging the gap between multi-view constraints and perceptual 3D understanding. This approach opens new possibilities for generating semantically rich and visually engaging 3D designs.
- Our method enables the creation of high-quality meshes with detailed textures, superior geometry, intricate designs, and smooth transitions—all from just a few prompts. Furthermore, the results produced by our approach are fabricable and do not rely on specific setups, significantly enhancing their practical value and broadening their potential applications.

## 2 Related work

*Shape from X.* The previous works in the “Shape from X” series primarily focus on high-precision reconstruction of existing objects based on known specific visual data, such as RGB images [Goesele et al. 2007; Moulon et al. 2013; Schönberger and Frahm 2016; Snavely et al. 2006; Wang et al. 2021], depth [Dai et al. 2017; Newcombe et al. 2011] and normals [Cao et al. 2022; Kadambi et al. 2015].

Constructing a single fixed object with multiple visual interpretations is a widely explored topic within the “Shape from X” domain. Researchers have explored a variety of methods to achieve diverse visual perceptions, leveraging factors such as viewing distance [Oliva et al. 2006], figure-ground organization [Kuo et al. 2017], illumination from different directions [Alexa and Matusik 2010; Baran et al. 2012; Bermano et al. 2012], light reflections [Sakurai et al. 2018; Wu et al. 2022], viewing angles [Hsiao et al. 2018; Qu et al. 2024; Sela and Elber 2007; Tojo et al. 2024; Zeng et al. 2021], and shadow casting on external planar surfaces [Mitra and Pauly 2009; Sadekar et al. 2022]. However, the goal of the above works is to produce different 2D information perceptions based on an object, whether it is a contour [Hsiao et al. 2018; Qu et al. 2024; Tojo et al. 2024], a projection [Mitra and Pauly 2009; Sadekar et al. 2022], or a picture [Min et al. 2017; Schwartzburg et al. 2014; Wu et al. 2022]. Our work differs in that it provides direct 3D information perception, allowing the characteristics of 3D objects to be experienced firsthand. To the best of our knowledge, no work has yet explored creating multiple 3D interpretations of a single object. In addition, we leverage semantics as a substitute for traditional inputs, similar to [Tojo et al. 2024] and [Qu et al. 2024], significantly expanding the creative space.

*3D Data Representations.* The expression of 3D data is a core topic in computer graphics and vision. Besides traditional point cloud and

mesh representations, neural implicit functions [Mescheder et al. 2019; Mildenhall et al. 2021; Park et al. 2019; Wang et al. 2021] and 3D Gaussian Splatting (3DGS) [Kerbl et al. 2023] have shown great advantages in various tasks recently. Mildenhall et al. proposed Neural Radiance Fields (NeRF) that represent a scene with a neural implicit function guided by neural rendering [Mildenhall et al. 2021]. This method has been widely applied to multi-view reconstruction [Li et al. 2023c; Wang et al. 2021, 2023a], sparse reconstruction [Jain et al. 2021; Liu et al. 2023; Niemeyer et al. 2022; Wynn and Turmukhambetov 2023; Yu et al. 2021], and generation tasks [Chen et al. 2023; Jain et al. 2022; Lin et al. 2023; Poole et al. 2022; Tang et al. 2023b; Wang et al. 2023b], thanks to its capability in representing scenes with rich details. However, its optimization process can be time-consuming and computationally intensive. Recent work on speeding up NeRF have mainly focused on improving rendering [Hedman et al. 2021; Li et al. 2023b; Reiser et al. 2021, 2023] and reconstruction speeds [Li et al. 2023c; Wang et al. 2023a], with only a few works applied to 3D generation [Li et al. 2023d].

At present, 3DGS [Kerbl et al. 2023], as a new 3D data expression, brings new possibilities for rendering [Lu et al. 2024; Yan et al. 2024; Yu et al. 2024a] and reconstruction problems [Fu et al. 2024; Guédon and Lepetit 2024; Luiten et al. 2024; Zhu et al. 2023] due to the fast optimization brought by flexible model design and efficient differentiable rendering framework. Furthermore, Tang et al. incorporated a generative model into 3DGS for 3D generation tasks, enabling generation of textured meshes [Tang et al. 2023a]. However, the geometry generated by 3DGS often suffers from significant detail loss, excessive surface undulations, and suboptimal mesh quality. We integrate these two promising 3D representations in our pipeline to produce innovative and manufacturable geometries.

*Diffusion Models in Vision.* In recent years, generative models have gained widespread attention in computer vision and graphics. They have achieved remarkable success in 2D generation for a wide range of tasks, including generating detailed images from rough ones [Lin et al. 2024; Tao Yang and Zhang 2023; Wang et al. 2024c; Yu et al. 2024b] and prompts [Ramesh et al. 2022; Rombach et al. 2022; Saharia et al. 2024], and creating videos from images [Sun et al. 2024; Yu et al. 2024c], estimating depths, normals [He et al. 2024; Yang et al. 2024a,b; Ye et al. 2024] and viewpoints [Wang et al. 2023c, 2024a]. On the other hand, 3D generation presents unique challenges, due to the limited availability of large, high-quality 3D datasets [Deitke et al. 2023, 2022; Koch et al. 2019; Wu et al. 2023]. Recently, most 3D generation methods [Chen et al. 2023; Jain et al. 2022; Lin et al. 2023; Poole et al. 2022; Tang et al. 2023b; Wang et al. 2023b] utilized 2D information as supervision to guide 3D generation, using neural implicit function as the primary representation of 3D data. DreamFields [Jain et al. 2022] pioneered the use of diffusion models for semantic-based 3D generation. DreamFussion [Poole et al. 2022] introduced the score distillation sampling (SDS) loss, which leverages semantic information and 2D rendering results, and this approach has since been widely adopted. DreamGaussian [Tang et al. 2023a] used 3DGS to represent 3D data, significantly improving generation speed. However, as these methods inherently rely on supervision from 2D rendering results, they often face challenges with multi-view inconsistency. While many existing works aim to mitigate

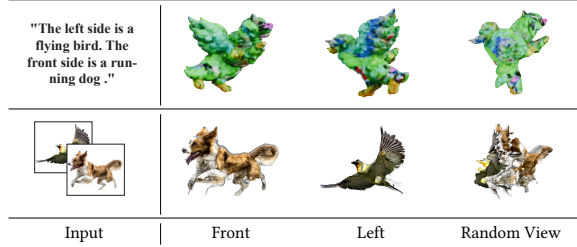


Fig. 2. **Failure of Naive Solutions.** We conduct direct text-to-3D or text-to-image-to-3D approaches to solve the proposed problem. However, these solutions have significant deficiencies in semantic understanding and geometric consistency. Our result of this case can be found in Fig. 11.

such inconsistencies [Liu et al. 2023; Shi et al. 2023], our approach leverages such potential inconsistency to generate creative objects with multiple visual interpretations. Moreover, researchers incorporate various priors (normal, depth, etc.) into 3D generation tasks to enhance the realism of models. SweetDreamer [Li et al. 2023a] and RichDreamer [Qiu et al. 2024] integrate canonical coordinate maps and normal-depth priors into the loss function, respectively. Meanwhile, Wonder3D [Long et al. 2023] and CRM [Wang et al. 2024b] directly utilize these priors to construct corresponding meshes.

### 3 Method

Our input consists of  $n$  semantic labels  $\mathcal{T} = \{t_i\}$  where each  $t_i$  represents a textual prompt, along with their corresponding view directions  $\mathcal{V} = \{v_i\}$  with  $v_i \in \text{SO}(3)$ . We refer to  $\mathcal{V}$  as the primary views, which can either be predefined or initialized randomly. Our purpose is to generate a colored 3D shape  $\mathcal{S}$  such that its texture and geometry when observed from any primary view align with the associated semantic class. Formally, this can be expressed as:

$$\min_{\mathcal{S}} \mathcal{L}_{\text{reg}}(\mathcal{S}), \quad \text{s.t. } P(\mathcal{S}, v_i) \in C(t_i), \quad i = 1, \dots, n, \quad (1)$$

where  $P(\mathcal{S}, v_i)$  denotes the appearance of  $\mathcal{S}$  when observed from the direction  $v_i$ , and  $C(t_i)$  denotes the class of images consistent with the prompt  $t_i$ .  $\mathcal{L}_{\text{reg}}$  is a regularization loss that enforces the following conditions for  $\mathcal{S}$  in addition to the semantic constraints:

- *Efficient Structure:* The design of  $\mathcal{S}$  should be simple, intuitive, and compact to facilitate fabrication while maintaining geometric features that contribute to its appearance.
- *Natural Transitions:* The parts of  $\mathcal{S}$  corresponding to each semantics should transition smoothly in both color and shape. This helps to generate aesthetically appealing results not only for the primary views but also for adjacent views.
- *Aesthetic Appeal:* The generated shape should be highly recognizable and visually elegant.

Designing a visually appealing and semantically consistent 3D shape requires substantial creativity and imagination. Although recent advancements in generative models provide a powerful foundation for addressing this challenge, directly using such models often produces unsatisfactory results. As shown in the top row of Fig. 2, existing text-to-3D models like DreamGaussian [Tang et al. 2023a] struggle to generate 3D shapes from text prompts that

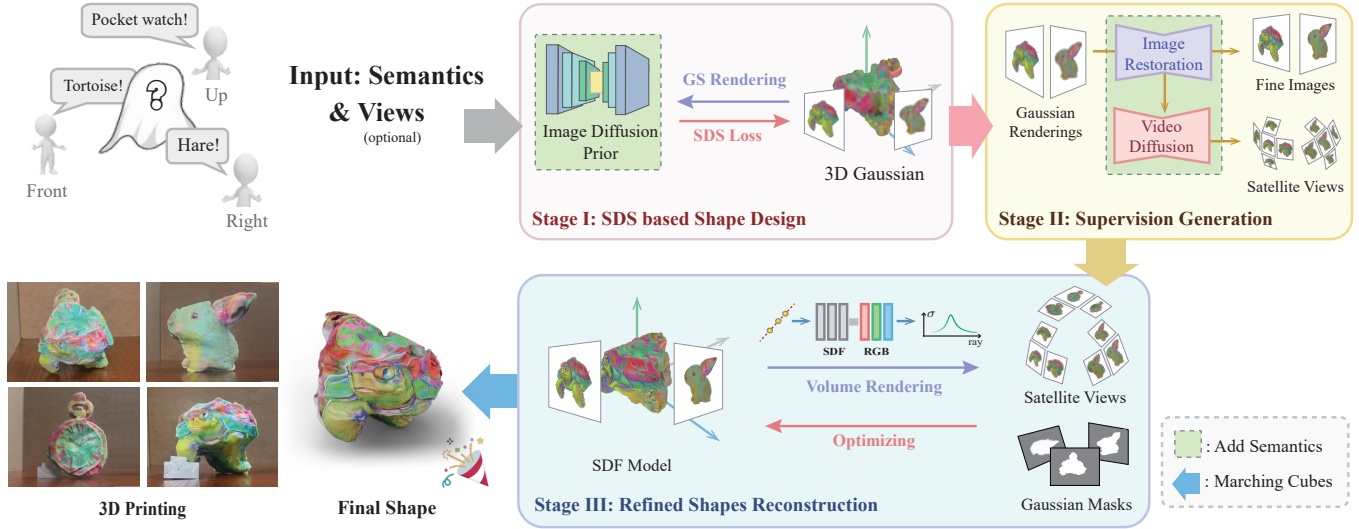


Fig. 3. **Shape from Semantics Pipeline.** For given semantics, we first adopt a 2D generative model to supervise and design a rough geometric shape, and then use diffusion models for image restoration and video generation to generate more high-quality images. Finally, we use SDF representation to reconstruct the detailed shape under the supervision of generated images and Gaussian masks. Our shape is fabricable and can be produced by 3D printing.

describe different semantics under different view directions. This might be because the same prompt are used to describe the orientation in supervision of different views, which makes it ambiguous. At the same time, generating additional elements in shapes does not seriously violate the semantics, making undesirable blending of all semantics into a single object a trivial solution. Alternatively, one could first generate an image for each semantic label using a text-to-image model such as Stable Diffusion 3.5 [Esser et al. 2024], and then use the generated images as input to create a 3D shape with multi-view reconstruction. However, as shown in the bottom row of Fig. 2, such an approach can lead to an unnatural transition of geometry between the primary view directions. This is because each image is generated independently, which fail to ensure the compatibility of their corresponding geometry on the final shape.

We propose to gradually generate the geometry and appearance from multi-view semantics in a structure-to-detail manner in three stages with the help of generative models (see Fig. 3). First, we leverage 2D generative priors to design the overall structure of the shape. Next, we use an image restoration model to improve the quality of rendered images, and use a video diffusion model to produce additional views based on the rendered results, which serve as supervision for subsequent optimization. Finally, we train a neural signed distance function that represents the refined shape with detailed geometry and texture, and extract a mesh surface from it as the final fabricable result.

### 3.1 Multi-Semantics SDS based Shape Design

Designing the structure of the shape is key to the entire task, as it directly affects the smoothness of transition between different views. To this end, we utilize generative models capable of understanding semantics. While recent 3D generation techniques can generate more realistic shapes, they are typically based on 3D consistency

priors to create a globally consistent shape from a single semantic. In contrast, since our input semantics describe different objects, we need to allow for 3D inconsistencies between different views to accommodate multiple semantics in a single object. Therefore, we follow [Poole et al. 2022; Wang et al. 2023b] and adopt the Score Distillation Sampling (SDS) loss to supervise the generation of 3D shapes through a text-to-image model, and extend the SDS process to our multi-semantics case. Using this loss, we optimize a coarse shape represented using 3D Gaussian Splatting.

*Multi-Semantics SDS Loss.* We choose Stable Diffusion [Rombach et al. 2022] as our 2D prior. In each iteration, for each semantics  $t_i$ , we randomly sample a camera pose  $p_i$  around its primary view  $v_i$  and render an RGB image  $I_i$  of the current view. Then  $I_i$  is input into the text-to-image model as the image to be denoised. For each  $I_i$ , we compute the gradient of original SDS loss with respect to  $\Theta$ , the parameters that encode  $\mathcal{S}$ , with semantics  $t_i$ :

$$\nabla_{\Theta} \mathcal{L}_{\text{SDS}}(t_i) = \mathbb{E}_{t, \epsilon} \left[ w(t) \left( \epsilon_{\phi}(I_i; t, e_i) - \epsilon \right) \frac{\partial I_i}{\partial \Theta} \right], \quad (2)$$

where  $\epsilon_{\phi}$  and  $\epsilon$  are the predicted and added noise respectively, and  $e_i$  is the CLIP embeddings of  $t_i$ . Note that our sampled camera poses  $\{p_i\}$  can deviate from the primary views, which brings two advantages. First, it ensures that geometric shapes maintain their intended semantics even when not strictly observed from the primary view directions to make our generated geometries without texture should also look meaningful. Moreover, expanding the camera’s selection range allows capturing more overlapping regions between different semantics in  $\mathcal{S}$  during rendering, thereby enabling the SDS process to facilitate natural transitions between adjacent parts better. Then, the gradient of multi-semantics SDS loss is defined as the average

loss under different semantics:

$$\nabla_{\Theta} \mathcal{L}_{\text{SDS}}(\mathcal{S}) = \frac{1}{n} \sum_{i=1}^n \nabla_{\Theta} \mathcal{L}_{\text{SDS}}(t_i). \quad (3)$$

**3D Gaussian Splatting Representation.** 3D Gaussian Splatting (3DGS) [Kerbl et al. 2023; Tang et al. 2023a] is an efficient 3D modeling method that represents scenes as a collection of Gaussian primitives. Each Gaussian primitive represents a 3D Gaussian distribution and is represented with the following components: the center  $\mathbf{x} \in \mathbb{R}^3$ , a scaling factor  $\mathbf{s} \in \mathbb{R}^3$ , a rotation quaternion  $\mathbf{q} \in \mathbb{R}^4$ , an opacity value  $\alpha \in \mathbb{R}$  and a color feature  $\mathbf{c} \in \mathbb{R}^3$ . To ensure that the shape color is independent of views in the final fabrication, spherical harmonics are disabled in our task. Therefore, the model parameter  $\Theta$  can be presented as:

$$\Theta = \{\Theta_k\} = \{\mathbf{x}_k, \mathbf{s}_k, \mathbf{q}_k, \alpha_k, \mathbf{c}_k\}. \quad (4)$$

To render 3D Gaussians into images, the primitives are first projected onto the image plane. Then, volume rendering is applied to each pixel in front-to-back order based on depth to compute the final color and alpha values. Compared to other representations, the results generated with 3DGS guided by SDS capture semantic information more effectively, render faster, and exhibit fewer failure cases. We observe that regions of different semantics within the same shape tend to adopt similar color styles (see Fig. 3, the green tortoise and hare), which facilitates smooth transitions between regions. Moreover, the unstructured nature of 3DGS makes it more flexible in representing 3D shapes with different topologies, which is highly suitable for our creative task. To enforce the structure efficiency required in Eq. (1), we penalize the standard deviation  $\sigma(\cdot)$  of the depth value  $d_i(\cdot)$  for the Gaussian centers  $\{\mathbf{x}_k\}$  under each primary view  $v_i$  to keep the overall volume compact:

$$\mathcal{L}_{\text{reg}} = \sum_i \sigma(\{d_i(\mathbf{x}_k)\}), \quad (5)$$

The total loss is:

$$\mathcal{L} = \mathcal{L}_{\text{SDS}} + \lambda \mathcal{L}_{\text{reg}}. \quad (6)$$

At this stage, we have obtained a shape that generally meets the requirements of Eq. (1). However, it still lacks sufficient details. Therefore, we subsequently use more generative models to introduce additional details based on the 3DGS results, which in turn guide the optimization of a more refined shape.

### 3.2 Generation of Detailed and Multi-View Supervision

We augment the details based on Gaussian renderings from  $n$  primary views, as they best represent the visuals and geometric features of  $\mathcal{S}$ . These renderings currently have certain limitations: insufficient image clarity and a limited number of views. Therefore, we utilize corresponding generative models to address these issues.

*Improving Resolution through Image Restoration.* Although the rendering of Gaussians in the first stage is blurry, it guides the overall shape structure and how different parts merge together. Therefore, it is necessary to refine the rendering while maintaining the original image structure and color style. To achieve this goal, we adopt the image restoration work SUPIR [Yu et al. 2024b]. We input the Gaussian rendering images from the primary views into the model to obtain the restored images, and provide semantic guidance in this process to ensure that the result makes sense.



Fig. 4. **Example for Image Restoration.** Prompt: "A detailed waterfall".

*Generating Satellite-view Images.* The generated high-quality images are insufficient to provide comprehensive constraints. Thus, alternative methods are required to supervise the geometry of various semantics effectively. A straightforward approach is leveraging depth or normal estimation [He et al. 2024; Yang et al. 2024a,b; Ye et al. 2024] or employing image-to-3D model techniques [Tang et al. 2024; Xiang et al. 2024]. However, due to the property of our task, geometry in a specific view must consider the influence of surrounding semantics and make certain deformations to adapt accordingly. Consequently, constraining geometry one view at a time proves overly rigid and may lead to geometric inconsistencies.

Compared to direct supervision methods, a more flexible alternative is to use images captured near the primary views for supervision. This approach offers the advantage of adjustable supervision scope, achieved by controlling the viewing angles of the capturing camera. Additionally, supervision intensity can be reduced for areas farther from the primary viewpoint by adding weights, enabling compatibility across different semantic geometries. We employ DimensionX [Sun et al. 2024] to accomplish this task. The restored images are fed into the model, guided by semantics, to generate videos simulating camera movement around the primary views. Subsequently, Dust3R [Wang et al. 2024a] is used to estimate the camera parameters for each frame of the generated video. Due to the continuity between video frames, the geometry generated within a small angular range achieves better consistency than models like zero-123 [Liu et al. 2023]. These surrounding views, termed as *satellite views*, provide abundant geometric information when used as supervision later on, proving particularly effective for representing convex geometric structures, as illustrated in Fig. 5.

### 3.3 Reconstruction of Refined Shapes with Neural SDF

In the final stage, we derive a more refined shape  $\mathcal{S}$  under the supervision of previous results. Since the multi-view images already contain sufficient semantic information, we only consider reconstruction at this stage. We use the neural implicit SDF function  $\mathcal{F}$  as the shape representation to benefit from its capability to represent detailed geometric shapes and easily calculate geometric information such as normals. To achieve high-quality rendering, we follow the SDF-based volume rendering framework [Mildenhall et al. 2021; Wang et al. 2021], using an SDF network for geometry and an RGB network for color presentation. During rendering, we collect rays from both the primary views and satellite views, and use the volume rendering formula to calculate the color loss for each ray:

$$\mathcal{L}_{\text{rgb}} = \|\hat{C} - C\|, \quad \hat{C} = \sum_{k=1}^n \alpha_k c_k \prod_{l=1}^{k-1} (1 - \alpha_l), \quad (7)$$

where  $\alpha_k$  is the opacity derived from the SDF values of sample points along the ray, and  $c_k$  is predicted by the color network. For satellite

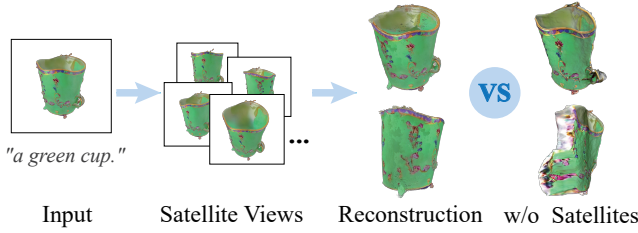


Fig. 5. **Example for Satellite Views.** During reconstruction in the third stage, the generated satellite-view images can mitigate geometric flattening.

views, to lead to natural shape transition, we design additional weights for each satellite view light when calculating the loss:

$$w_{i,j} = \exp(-\mu \sin \langle v_{i,j}, v_i \rangle), \quad (8)$$

where  $v_{i,j}$  is the  $j$ -th satellite view of  $v_i$ , and  $\mu$  is a hyperparameter. In this way, images farther from the primary view will have less influence on the regions corresponding to other semantics, helping to avoid geometric incompatibility.

In addition, to leverage the geometric features of the first stage without introducing local inaccuracies, we sample a set of camera poses to render opacity images of 3DGS. These images were used as masks to guide the optimization of SDF, ensuring that the cumulative opacity along each ray closely aligns with the mask values. This strategy ensures the overall structure remains reasonable while allowing the SDF sufficient flexibility for detail refinement. Meanwhile, since the supervised view focuses on areas near the primary view, less captured regions often appear overly compact and deflated. To address this, we introduce a dilation loss on a random point set  $P$  near the surface to make the overall geometry well-rounded:

$$\mathcal{L}_{\text{dil}} = \frac{1}{|P|} \sum_{p \in P} \max\{\mathcal{F}(p), 0\}. \quad (9)$$

We give it a lower weight to ensure the overall structure remains efficient. In addition, eikonal loss [Gropp et al. 2020]  $\mathcal{L}_{\text{eik}}$  is adopted to maintain  $\|\nabla \mathcal{F}\| = 1$ . The regularization loss term is:

$$\mathcal{L}_{\text{reg}} = \gamma_1 \mathcal{L}_{\text{dil}} + \gamma_2 \mathcal{L}_{\text{eik}}. \quad (10)$$

In summary, our loss in this stage is:

$$\mathcal{L} = \mathcal{L}_{\text{rgb}} + \alpha \mathcal{L}_{\text{mask}} + \beta \mathcal{L}_{\text{reg}}. \quad (11)$$

In this stage, the Gaussian masks and regularization loss make the structure of  $\mathcal{S}$  efficient, and the high-resolution images generated in the second stage ensure sufficient details and beautiful appearance. Since the generated supervision and the final reconstruction are loyal to the design in the first stage, the color and geometry of different parts of  $\mathcal{S}$  can transition naturally and conform to the semantics under the input primary views. At this point, we get the expected shape defined in Eq. (1). We then use the Marching Cubes algorithm [Lorensen and Cline 1987] to extract a mesh, and use the color network to add the color for mesh vertices. During the rendering process, in order to ensure the geometry extraction convenience, we make the color no longer related to the view directions but still related to the normals, so that the change of rendering will also

Table 1. **CLIP Similarity (%) (higher is better) between the Semantics and the Observed Meshes.** The indices here are consistent with the ones in Fig. 7. Each result is displayed as scores of with/without textures. As a reference, the score for a semantically perfect image is around 41.

Index	View1	View2	View3	Mean Score
Case 1	38.00 / 36.39	35.94 / 32.35	33.40 / 36.49	35.78 / 35.07
Case 2	41.24 / 27.92	40.46 / 26.63	33.93 / 25.56	38.55 / 26.70
Case 3	40.07 / 23.42	33.86 / 28.26	37.17 / 28.86	37.03 / 26.85
Case 4	40.26 / 23.25	39.51 / 32.22	36.61 / 32.04	38.79 / 29.17
Case 5	39.03 / 37.36	37.81 / 36.62	36.92 / 34.27	37.92 / 36.08
Case 6	32.48 / 29.99	41.79 / 30.63	36.87 / 26.06	37.05 / 28.89
Case 7	39.41 / 23.17	38.21 / 36.69	39.09 / 33.83	38.90 / 31.23

lead to the change of local geometry fluctuations, thus producing a relief-sculpture-like effect.

## 4 Experiments

*Implementation Details.* In the first stage of our pipeline, we adopt the configuration of DreamGaussian [Tang et al. 2023a] and conduct training for 500 iterations. Each Gaussian is initialized as a sphere centered at  $(0, 0, 0)$ , while the cameras are distributed on a sphere with a radius of 2.5. During training, we randomly sample camera positions within a 20-degree range around each primary view. For image restoration, we employ the ComfyUI integrated version of SUPIR and directly input Gaussian renderings from the primary views. For video generation, we leverage the original code of DimensionX. We remove the background from the SUPIR results and input them into the model, selecting 20 frames closest to the primary view in the generated videos as satellite views. All experiments are conducted on an NVIDIA A100 (80GB) GPU, with the first and third stage training requiring less than 10 GB of GPU memory. The only exception is that when compared with other methods, we run Fantasia3D [Chen et al. 2023] using  $8 \times 3090$  GPUs, which is its official configuration. For the Marching Cubes Algorithm, we sample the SDF on a grid with a  $1024^3$  resolution. In the following parts, the case indexes in the tables refer to Fig. 7.

*Main Results.* We use our method to generate various multi-semantic textured meshes. The rendering results and normal maps are shown in Fig. 7. The meshes are created using diverse semantic and view inputs, demonstrating the rich creativity of our method. The outcomes align well with expected semantics in both geometry and rendering quality. To validate the manufacturability of the generated shapes, we 3D-printed several examples using both colored and white materials: the white prints make it easy to observe the geometric details, while the colored prints verify the final appearance. The results are shown in Fig. 10. The fabricated objects closely match the intended designs and exhibit an aesthetic appeal.

*Quantitative Evaluation.* To evaluate the consistency between the generated results and the input semantics, we render the generated shapes from various primary views and use the CLIP score [Radford et al. 2021] to measure their semantic similarity to the input. Table 1 presents the CLIP scores for textured and non-textured cases. For each primary view, we allow random variations within a

Table 2. **Scores of the User Study.** The indices here are consistent with the ones in Fig. 7. For each term, the rating range is 0-10, with higher scores indicating that our results are better.

Index	w/o Texture	w/ Texture	Semantic Pref.	Overall Pref.
Case 1	8.82	9.56	8.82	9.00
Case 2	4.52	7.57	8.14	8.16
Case 3	6.34	9.41	8.70	9.17
Case 4	7.45	9.54	8.22	8.96
Case 5	8.10	9.45	7.87	8.30
Case 6	3.89	8.64	8.24	8.34
Case 7	6.07	8.77	8.43	8.74

20-degree latitude and longitude range to render the images. The CLIP model then evaluates the captured results 1,000 times, and the average score is taken as the score for that primary view. The results indicate that the generated shapes effectively convey semantic information, regardless of whether textures are applied. Observers can also discern the semantic representation of these geometric shapes even with slight changes in perspective.

In addition, we conducted a user study to further validate our method. The participants were shown the rendering of our generated shapes one at a time, and asked to sequentially answer the following questions with a score from 0 to 10:

- Q1: How semantically accurate is our textureless rendering?
- Q2: How semantically accurate is our textured rendering?

The last two questions focus on participants’ preferences between the results of ours and [Tojo et al. 2024] under the same semantics. A score closer to 10 indicates a stronger preference for our results:

- Q3: Which result better aligns with semantics?
- Q4: Which overall result do you prefer?

We randomly and fairly selected participants, collecting 102 samples. The average scores from each primary view of each case are presented in Tab. 2. The results indicate that our shape design receives considerable recognition in terms of rendering quality. However, our geometry scores were relatively lower, likely due to the need to account for compatibility across different semantics. This might lead to a degree of shape deformation, which may have impacted realism. Nevertheless, in preference scoring, our overall performance in semantics and aesthetics is significantly higher compared to the methods we benchmarked against. This suggests that the combination of our rendering and geometry maintains strong semantic expressiveness. Moreover, when compared to monochrome or outline results, our overall design proved to be highly appealing.

*Qualitative Comparison.* As far as we know, no previous research has been conducted with the same purpose as ours. Therefore, we make comparisons with similar works like Shadow Art [Mitra and Pauly 2009] and Wire Art [Tojo et al. 2024]. Similar to us, they aim to represent diverse semantics from different views. Initially, we provided images after restoration to both of them and compared their results with our reconstruction. As shown in Fig. 12, both methods convey information solely through contours and silhouettes, lacking color representation and meaningful geometric expression. In contrast, our shape representation integrates rendering, enabling the depiction of more intricate and complex shapes while enhancing

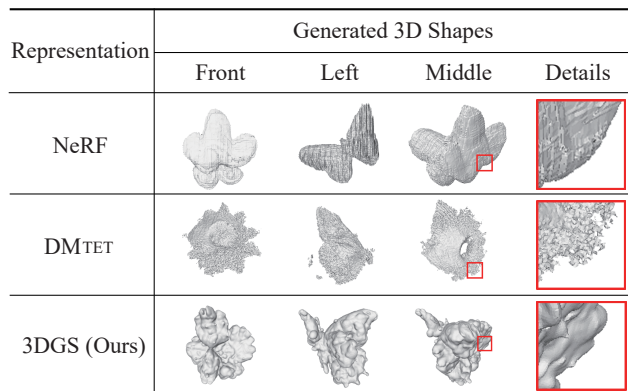


Fig. 6. **The Generation Results of Different Representations.** The input semantics are “a flower” & “a butterfly”. We compare with Dreamfusion [Tang 2022] using NeRF and Fantasia3D [Chen et al. 2023] using DMTEt [Shen et al. 2021], adding multiple-semantics SDS guidance to their frameworks. Results show that our 3DGS geometry is more stable and detailed. The fabrication result of our final model is presented in Fig. 10.

the presentation of geometry. Fig. 11 further illustrates our comparison with Wire Art under the same semantic inputs. While both approaches align with the given semantics, our generated shapes are more intricate and refined. Additionally, as shown in the first row of Fig. 11, our method can utilize the occlusion of sight to convey different semantics on the front and back, which is challenging for simpler representations based mainly on contours.

To demonstrate the advantages of 3D GS, we experiment with different 3D representations during the design stage. Results are shown in Fig. 6. Compared to 3DGS, designs of other methods appear relatively dull, with excessive local geometric noise. Additionally, they require significantly more computational resources and longer generation time than Gaussian. 3DGS’s flexible and efficient rendering makes it more suitable for our task.

We also conduct an ablation study to show the effectiveness of dilation loss and multi-view Gaussian mask loss in stage 3 reconstruction. As illustrated in Fig. 8, the absence of dilation loss leads to distorted local geometry. Meanwhile, without Gaussian mask constraints, the overall shape becomes excessively inflated.

## 5 Conclusion & Discussion

We proposed and addressed a novel problem: generating shapes from multi-view semantics. The core of our approach is to leverage generative models for design and optimization. Experimental results demonstrated that our method successfully produced impressive shapes that are aesthetically pleasing, semantically aligned with the input, and easy to manufacture.

Our method still has some limitations. Despite several strategies that have been designed to align geometry and semantics, satisfactory results cannot be guaranteed under all semantic conditions. As shown in Fig. 9, this case achieves semantic alignment in rendering, but their geometry remains suboptimal. One potential solution is to consider the primary views as optimizable parameters, allowing them to adjust moderately during the generation process. This could

enhance the compatibility of shapes with different semantics. We leave it for future work.

## References

- Marc Alexa and Wojciech Matusik. 2010. Reliefs as images. *ACM Trans. Graph.* 29, 4, Article 60 (July 2010), 7 pages. <https://doi.org/10.1145/1778765.1778797>
- Ilya Baran, Philipp Keller, Derek Bradley, Stelian Coros, Wojciech Jarosz, Derek Nowrouzezahrai, and Markus Gross. 2012. Manufacturing Layered Attenuators for Multiple Prescribed Shadow Images. *Comput. Graph. Forum* 31, 2pt3 (May 2012), 603–610. <https://doi.org/10.1111/j.1467-8659.2012.03039.x>
- Amit Bermano, Ilya Baran, Marc Alexa, and Wojciech Matusik. 2012. ShadowPix: Multiple Images from Self Shadowing. *Comput. Graph. Forum* 31, 2pt3 (May 2012), 593–602. <https://doi.org/10.1111/j.1467-8659.2012.03038.x>
- Xu Cao, Hiroaki Santo, Boxin Shi, Fumio Okura, and Yasuyuki Matsushita. 2022. Bilateral Normal Integration.
- Rui Chen, Yongwei Chen, Ningxin Jiao, and Kui Jia. 2023. Fantasia3D: Disentangling Geometry and Appearance for High-quality Text-to-3D Content Creation. In *Proceedings of the IEEE/CVF International Conference on Computer Vision (ICCV)*. 22246–22256.
- Angela Dai, Matthias Nießner, Michael Zollhöfer, Shahram Izadi, and Christian Theobalt. 2017. BundleFusion: Real-Time Globally Consistent 3D Reconstruction Using On-the-Fly Surface Reintegration. *ACM Trans. Graph.* 36, 3, Article 24 (May 2017), 18 pages. <https://doi.org/10.1145/3054739>
- Matt Deitke, Ruoshi Liu, Matthew Wallingford, Huong Ngo, Oscar Michel, Aditya Kusupati, Alan Fan, Christian Laforte, Vikram Voleti, Samir Yitzhak Gadre, Eli VanderBilt, Aniruddha Kembhavi, Carl Vondrick, Georgia Gkioxari, Kiana Ehsani, Ludwig Schmidt, and Ali Farhadi. 2023. Objaverse-XL: A Universe of 10M+ 3D Objects. *arXiv preprint arXiv:2307.05663* (2023).
- Matt Deitke, Dustin Schwenk, Jordi Salvador, Luca Weihs, Oscar Michel, Eli VanderBilt, Ludwig Schmidt, Kiana Ehsani, Aniruddha Kembhavi, and Ali Farhadi. 2022. Objaverse: A Universe of Annotated 3D Objects. *arXiv preprint arXiv:2212.08051* (2022).
- Patrick Esser, Sumith Kulal, Andreas Blattmann, Rahim Entezari, Jonas Müller, Harry Saini, Yam Levi, Dominik Lorenz, Axel Sauer, Frederic Boesel, et al. 2024. Scaling rectified flow transformers for high-resolution image synthesis. In *Forty-first International Conference on Machine Learning*.
- Yang Fu, Sifei Liu, Ameer Kulkarni, Jan Kautz, Alexei A. Efros, and Xiaocong Wang. 2024. COLMAP-Free 3D Gaussian Splatting. In *Proceedings of the IEEE/CVF Conference on Computer Vision and Pattern Recognition (CVPR)*. 20796–20805.
- Michael Goesele, Noah Snavely, Brian Curless, Hugues Hoppe, and Steven M. Seitz. 2007. Multi-View Stereo for Community Photo Collections. In *2007 IEEE 11th International Conference on Computer Vision*. 1–8. <https://doi.org/10.1109/ICCV.2007.4408933>
- Amos Gropp, Lior Yariv, Niv Haim, Matan Atzmon, and Yaron Lipman. 2020. Implicit Geometric Regularization for Learning Shapes. In *Proceedings of Machine Learning and Systems 2020*. 3569–3579.
- Antoine Guédon and Vincent Lepetit. 2024. SuGaR: Surface-Aligned Gaussian Splatting for Efficient 3D Mesh Reconstruction and High-Quality Mesh Rendering. *CVPR* (2024).
- Jing He, Haodong Li, Wei Yin, Yixun Liang, Leheng Li, Kaiqiang Zhou, Hongbo Liu, Bingbing Liu, and Ying-Cong Chen. 2024. Lotus: Diffusion-based Visual Foundation Model for High-quality Dense Prediction. *arXiv preprint arXiv:2409.18124* (2024).
- Peter Hedman, Pratul P. Srinivasan, Ben Mildenhall, Jonathan T. Barron, and Paul Debevec. 2021. Baking Neural Radiance Fields for Real-Time View Synthesis. *ICCV* (2021).
- Kai-Wen Hsiao, Jia-Bin Huang, and Hung-Kuo Chu. 2018. Multi-view Wire Art. *ACM Trans. Graph.* 37, 6, Article 242 (2018), 11 pages.
- Ajay Jain, Ben Mildenhall, Jonathan T. Barron, Pieter Abbeel, and Ben Poole. 2022. Zero-Shot Text-Guided Object Generation with Dream Fields. *CVPR* (2022).
- Ajay Jain, Matthew Tancik, and Pieter Abbeel. 2021. Putting NeRF on a Diet: Semantically Consistent Few-Shot View Synthesis. In *Proceedings of the IEEE/CVF International Conference on Computer Vision (ICCV)*. 5885–5894.
- Achuta Kadambi, Vage Taamazyan, Boxin Shi, and Ramesh Raskar. 2015. Polarized 3D: High-Quality Depth Sensing with Polarization Cues. In *2015 IEEE International Conference on Computer Vision (ICCV)*. 3370–3378. <https://doi.org/10.1109/ICCV.2015.385>
- Bernhard Kerbl, Georgios Kopanas, Thomas Leimkuehler, and George Drettakis. 2023. 3D Gaussian Splatting for Real-Time Radiance Field Rendering. *ACM Trans. Graph.* 42, 4, Article 139 (July 2023), 14 pages. <https://doi.org/10.1145/3592433>
- Sebastian Koch, Albert Matveev, Zhongshi Jiang, Francis Williams, Alexey Artemov, Evgeny Burnaev, Marc Alexa, Denis Zorin, and Daniele Panozzo. 2019. ABC: A Big CAD Model Dataset For Geometric Deep Learning. In *The IEEE Conference on Computer Vision and Pattern Recognition (CVPR)*.
- Ying-Miao Kuo, Hung-Kuo Chu, Ming-Te Chi, Ruen-Rone Lee, and Tong-Yee Lee. 2017. Generating Ambiguous Figure-Ground Images. *IEEE Transactions on Visualization and Computer Graphics* 23, 5 (2017), 1534–1545. <https://doi.org/10.1109/TVCG.2016.2535331>
- Jiahao Li, Hao Tan, Kai Zhang, Zexiang Xu, Fujun Luan, Yinghao Xu, Yicong Hong, Kalyan Sunkavalli, Greg Shakhnarovich, and Sai Bi. 2023d. Instant3D: Fast Text-to-3D with Sparse-View Generation and Large Reconstruction Model. <https://arxiv.org/abs/2311.06214> (2023).
- Sixu Li, Chaojian Li, Wenbo Zhu, Boyang (Tony) Yu, Yang (Katie) Zhao, Cheng Wan, Haoran You, Huihong Shi, and Yingyan (Celine) Lin. 2023b. Instant-3D: Instant Neural Radiance Field Training Towards On-Device AR/VR 3D Reconstruction. In *Proceedings of the 50th Annual International Symposium on Computer Architecture (Orlando, FL, USA) (ISCA '23)*. Association for Computing Machinery, New York, NY, USA, Article 6, 13 pages. <https://doi.org/10.1145/3579371.3589115>
- Weiyu Li, Rui Chen, Xuelin Chen, and Ping Tan. 2023a. SweetDreamer: Aligning Geometric Priors in 2D Diffusion for Consistent Text-to-3D. *arXiv:2310.02596* (2023).
- Zhaoshuo Li, Thomas Müller, Alex Evans, Russell H Taylor, Mathias Unberath, Ming-Yu Liu, and Chen-Hsuan Lin. 2023c. Neuralangelo: High-Fidelity Neural Surface Reconstruction. In *IEEE Conference on Computer Vision and Pattern Recognition (CVPR)*
- Chen-Hsuan Lin, Jun Gao, Luming Tang, Towaki Takikawa, Xiao-hui Zeng, Xun Huang, Karsten Kreis, Sanja Fidler, Ming-Yu Liu, and Tsung-Yi Lin. 2023. Magic3D: High-Resolution Text-to-3D Content Creation. In *IEEE Conference on Computer Vision and Pattern Recognition (CVPR)*.
- Xinqi Lin, Jingwen He, Ziyang Chen, Zhaoyang Lyu, Bo Dai, Fanghua Yu, Wanli Ouyang, Yu Qiao, and Chao Dong. 2024. DiffBIR: Towards Blurry Blind Image Restoration with Generative Diffusion Prior. *arXiv:2308.15070* [cs.CV]
- Ruoshi Liu, Rundi Wu, Basile Van Hoorick, Pavel Tokmakov, Sergey Zakharov, and Carl Vondrick. 2023. Zero-1-to-3: Zero-shot One Image to 3D Object. *arXiv:2303.11328* [cs.CV]
- Xiaoxiao Long, Yuan-Chen Guo, Cheng Lin, Yuan Liu, Zhiyang Dou, Lingjie Liu, Yuexin Ma, Song-Hai Zhang, Marc Habermann, Christian Theobalt, et al. 2023. Wonder3D: Single Image to 3D using Cross-Domain Diffusion. *arXiv preprint arXiv:2310.15008* (2023).
- William E. Lorensen and Harvey E. Cline. 1987. Marching cubes: A high resolution 3D surface construction algorithm. In *Proceedings of the 14th Annual Conference on Computer Graphics and Interactive Techniques (SIGGRAPH '87)*. Association for Computing Machinery, New York, NY, USA, 163–169. <https://doi.org/10.1145/37401.37422>
- Tao Lu, Mulin Yu, Linning Xu, Yuanbo Xiangli, Limin Wang, Dahua Lin, and Bo Dai. 2024. Scaffold-3d: Structured 3d gaussians for view-adaptive rendering. In *Proceedings of the IEEE/CVF Conference on Computer Vision and Pattern Recognition*. 20654–20664.
- Jonathan Luiten, Georgios Kopanas, Bastian Leibe, and Deva Ramanan. 2024. Dynamic 3D Gaussians: Tracking by Persistent Dynamic View Synthesis. In *3DV*.
- Lars Mescheder, Michael Oechsle, Michael Niemeyer, Sebastian Nowozin, and Andreas Geiger. 2019. Occupancy Networks: Learning 3D Reconstruction in Function Space. In *Proceedings of the IEEE/CVF Conference on Computer Vision and Pattern Recognition (CVPR)*.
- Ben Mildenhall, Pratul P Srinivasan, Matthew Tancik, Jonathan T Barron, Ravi Ramamoorthi, and Ren Ng. 2021. Nerf: Representing scenes as neural radiance fields for view synthesis. *Commun. ACM* 65, 1 (2021), 99–106.
- Sehee Min, Jaedong Lee, Jungdam Won, and Jehee Lee. 2017. Soft Shadow Art. In *Computational Aesthetics*, Holger Winnemoeller and Lyn Bartram (Eds.). Association for Computing Machinery, Inc (ACM). <https://doi.org/10.1145/3092912.3092915>
- Niloy J. Mitra and Mark Pauly. 2009. Shadow art. In *ACM SIGGRAPH Asia 2009 Papers (Yokohama, Japan) (SIGGRAPH Asia '09)*. Association for Computing Machinery, New York, NY, USA, Article 156, 7 pages. <https://doi.org/10.1145/1661412.1618502>
- Pierre Moulon, Pascal Monasse, and Renaud Marlet. 2013. Global Fusion of Relative Motions for Robust, Accurate and Scalable Structure from Motion. In *2013 IEEE International Conference on Computer Vision*. 3248–3255. <https://doi.org/10.1109/ICCV.2013.403>
- Richard A. Newcombe, Shahram Izadi, Otmar Hilliges, David Molyneaux, David Kim, Andrew J. Davison, Pushmeet Kohi, Jamie Shotton, Steve Hodges, and Andrew Fitzgibbon. 2011. KinectFusion: Real-time dense surface mapping and tracking. In *2011 10th IEEE International Symposium on Mixed and Augmented Reality*. 127–136. <https://doi.org/10.1109/ISMAR.2011.6092378>
- Michael Niemeyer, Jonathan T. Barron, Ben Mildenhall, Mehdi S. M. Sajjadi, Andreas Geiger, and Noha Radwan. 2022. RegNeRF: Regularizing Neural Radiance Fields for View Synthesis from Sparse Inputs. In *Proc. IEEE Conf. on Computer Vision and Pattern Recognition (CVPR)*.
- Aude Oliva, Antonio Torralba, and Philippe G. Schyns. 2006. Hybrid images. *ACM Trans. Graph.* 25, 3 (July 2006), 527–532. <https://doi.org/10.1145/1141911.1141919>
- Jeong Joon Park, Peter R. Florence, Julian Straub, Richard A. Newcombe, and S. Lovegrove. 2019. DeepSDF: Learning Continuous Signed Distance Functions for Shape Representation. *2019 IEEE/CVF Conference on Computer Vision and Pattern Recognition (CVPR)* (2019), 165–174. <https://api.semanticscholar.org/CorpusID:58007025>
- Ben Poole, Ajay Jain, Jonathan T. Barron, and Ben Mildenhall. 2022. DreamFusion: Text-to-3D using 2D Diffusion. *arXiv* (2022).

- Lingteng Qiu, Guanying Chen, Xiaodong Gu, Qi Zuo, Mutian Xu, Yushuang Wu, Weihao Yuan, Zilong Dong, Liefeng Bo, and Xiaoguang Han. 2024. RichDreamer: A generalizable normal-depth diffusion model for detail richness in text-to-3d. In *Proceedings of the IEEE/CVF Conference on Computer Vision and Pattern Recognition*. 9914–9925.
- Zhiyu Qu, Lan Yang, Honggang Zhang, Tao Xiang, Kaiyue Pang, and Yi-Zhe Song. 2024. Wired Perspectives: Multi-View Wire Art Embraces Generative AI. In *CVPR*.
- Alec Radford, Jong Wook Kim, Chris Hallacy, Aditya Ramesh, Gabriel Goh, Sandhini Agarwal, Girish Sastry, Amanda Askell, Pamela Mishkin, Jack Clark, et al. 2021. Learning transferable visual models from natural language supervision. In *International conference on machine learning*. PMLR, 8748–8763.
- Aditya Ramesh, Prafulla Dhariwal, Alex Nichol, Casey Chu, and Mark Chen. 2022. Hierarchical Text-Conditional Image Generation with CLIP Latents. arXiv:2204.06125 [cs.CV] <https://arxiv.org/abs/2204.06125>
- Christian Reiser, Songyou Peng, Yiyi Liao, and Andreas Geiger. 2021. KiloNeRF: Speeding up Neural Radiance Fields with Thousands of Tiny MLPs. In *International Conference on Computer Vision (ICCV)*.
- Christian Reiser, Richard Szeliski, Dor Verbin, Pratul P. Srinivasan, Ben Mildenhall, Andreas Geiger, Jonathan T. Barron, and Peter Hedman. 2023. MERF: Memory-Efficient Radiance Fields for Real-time View Synthesis in Unbounded Scenes. *SIGGRAPH* (2023).
- Robin Rombach, Andreas Blattmann, Dominik Lorenz, Patrick Esser, and Bjorn Ommer. 2022. High-Resolution Image Synthesis with Latent Diffusion Models. In *2022 IEEE/CVF Conference on Computer Vision and Pattern Recognition (CVPR)*. IEEE Computer Society, Los Alamitos, CA, USA, 10674–10685. <https://doi.org/10.1109/CVPR52688.2022.01042>
- Kaustubh Sadekar, Ashish Tiwari, and Shanmuganathan Raman. 2022. Shadow Art Revisited: A Differentiable Rendering Based Approach. In *Proceedings of the IEEE/CVF Winter Conference on Applications of Computer Vision (WACV)*. 29–37.
- Chitwan Saharia, William Chan, Saurabh Saxena, Lala Lit, Jay Whang, Emily Denton, Seyed Kamyar Seyed Ghasemipour, Burcu Karagol Ayan, S. Sara Mahdavi, Raphael Gontijo-Lopes, Tim Salimans, Jonathan Ho, David J Fleet, and Mohammad Norouzi. 2024. Photorealistic text-to-image diffusion models with deep language understanding. In *Proceedings of the 36th International Conference on Neural Information Processing Systems (New Orleans, LA, USA) (NIPS '22)*. Curran Associates Inc., Red Hook, NY, USA, Article 2643, 16 pages.
- Kaisei Sakurai, Yoshinori Dobashi, Kei Iwasaki, and Tomoyuki Nishita. 2018. Fabricating reflectors for displaying multiple images. *ACM Trans. Graph.* 37, 4, Article 158 (July 2018), 10 pages. <https://doi.org/10.1145/3197517.3201400>
- Yuliy Schwartzburg, Romain Testuz, Andrea Tagliasacchi, and Mark Pauly. 2014. High-contrast computational caustic design. *ACM Trans. Graph.* 33, 4, Article 74 (July 2014), 11 pages. <https://doi.org/10.1145/2601097.2601200>
- Johannes L. Schönberger and Jan-Michael Frahm. 2016. Structure-from-Motion Revisited. In *2016 IEEE Conference on Computer Vision and Pattern Recognition (CVPR)*. 4104–4113. <https://doi.org/10.1109/CVPR.2016.445>
- Guy Sela and Gershon Elber. 2007. Generation of view dependent models using free form deformation. *Vis. Comput.* 23, 3 (Feb. 2007), 219–229. <https://doi.org/10.1007/s00371-006-0095-2>
- Tianchang Shen, Jun Gao, Kangxue Yin, Ming-Yu Liu, and Sanja Fidler. 2021. Deep Marching Tetrahedra: a Hybrid Representation for High-Resolution 3D Shape Synthesis. In *Advances in Neural Information Processing Systems (NeurIPS)*.
- Yichun Shi, Peng Wang, Jianglong Ye, Long Mai, Kejie Li, and Xiao Yang. 2023. MV-Dream: Multi-view Diffusion for 3D Generation. arXiv:2308.16512 (2023).
- Noah Snavely, Steven M. Seitz, and Richard Szeliski. 2006. Photo tourism: exploring photo collections in 3D. *ACM Trans. Graph.* 25, 3 (July 2006), 835–846. <https://doi.org/10.1145/1141911.1141964>
- Wenqiang Sun, Shuo Chen, Fangfu Liu, Zilong Chen, Yueqi Duan, Jun Zhang, and Yikai Wang. 2024. DimensionX: Create Any 3D and 4D Scenes from a Single Image with Controllable Video Diffusion. arXiv preprint arXiv:2411.04928 (2024).
- Jiaxiang Tang. 2022. Stable-dreamfusion: Text-to-3D with Stable-diffusion. <https://github.com/ashawkey/stable-dreamfusion>.
- Jiaxiang Tang, Zhaoxi Chen, Xiaokang Chen, Tengfei Wang, Gang Zeng, and Ziwei Liu. 2024. LGM: Large Multi-View Gaussian Model for High-Resolution 3D Content Creation. *ECCV* (2024).
- Jiaxiang Tang, Jiawei Ren, Hang Zhou, Ziwei Liu, and Gang Zeng. 2023a. DreamGaussian: Generative Gaussian Splatting for Efficient 3D Content Creation. arXiv preprint arXiv:2309.16653 (2023).
- Junshu Tang, Tengfei Wang, Bo Zhang, Ting Zhang, Ran Yi, Lizhuang Ma, and Dong Chen. 2023b. Make-It-3D: High-fidelity 3D Creation from A Single Image with Diffusion Prior. In *Proceedings of the IEEE/CVF International Conference on Computer Vision (ICCV)*. 22819–22829.
- Peiran Ren Xuansong Xie Tao Yang, Rongyuan Wu and Lei Zhang. 2023. Pixel-Aware Stable Diffusion for Realistic Image Super-Resolution and Personalized Stylization. In *The European Conference on Computer Vision (ECCV) 2024*.
- Kenji Tojo, Ariel Shamir, Bernd Bickel, and Nobuyuki Umetani. 2024. Fabricable 3D Wire Art. In *ACM SIGGRAPH 2024 Conference Papers* (Denver, CO, USA) (*SIGGRAPH '24*). Association for Computing Machinery, New York, NY, USA, Article 134, 11 pages. <https://doi.org/10.1145/3641519.3657453>
- Jianyuan Wang, Christian Rupprecht, and David Novotny. 2023c. PoseDiffusion: Solving Pose Estimation via Diffusion-aided Bundle Adjustment. *ICCV*.
- Jianyi Wang, Zongsheng Yue, Shangchen Zhou, Kelvin C.K. Chan, and Chen Change Loy. 2024c. Exploiting Diffusion Prior for Real-World Image Super-Resolution. (2024).
- Peng Wang, Lingjie Liu, Yuan Liu, Christian Theobalt, Taku Komura, and Wenping Wang. 2021. Neus: Learning neural implicit surfaces by volume rendering for multi-view reconstruction. arXiv preprint arXiv:2106.10689 (2021).
- Shuzhe Wang, Vincent Leroy, Yohann Cabon, Boris Chidlovskii, and Jerome Revaud. 2024a. DUST3R: Geometric 3D Vision Made Easy. In *Proceedings of the IEEE/CVF Conference on Computer Vision and Pattern Recognition (CVPR)*. 20697–20709.
- Yiming Wang, Qin Han, Marc Habermann, Kostas Daniilidis, Christian Theobalt, and Lingjie Liu. 2023a. NeuS2: Fast Learning of Neural Implicit Surfaces for Multi-view Reconstruction. In *Proceedings of the IEEE/CVF International Conference on Computer Vision (ICCV)*.
- Zhengyi Wang, Cheng Lu, Yikai Wang, Fan Bao, Chongxuan Li, Hang Su, and Jun Zhu. 2023b. ProlificDreamer: High-Fidelity and Diverse Text-to-3D Generation with Variational Score Distillation. arXiv preprint arXiv:2305.16213 (2023).
- Zhengyi Wang, Yikai Wang, Yifei Chen, Chendong Xiang, Shuo Chen, Dajiang Yu, Chongxuan Li, Hang Su, and Jun Zhu. 2024b. CRM: Single Image to 3D Textured Mesh with Convolutional Reconstruction Model. arXiv preprint arXiv:2403.05034 (2024).
- Kang Wu, Renjie Chen, Xiao-Ming Fu, and Ligang Liu. 2022. Computational Mirror Cup and Saucer Art. *ACM Trans. Graph.* 41, 5, Article 174 (July 2022), 15 pages. <https://doi.org/10.1145/3517120>
- Tong Wu, Jiarui Zhang, Xiao Fu, Yuxin Fang, Liang Pan Jiawei Ren, Wayne Wu, Lei Yang, Jiaqi Wang, Chen Qian, Dahua Lin, and Ziwei Liu. 2023. OmniObject3D: Large-Vocabulary 3D Object Dataset for Realistic Perception, Reconstruction and Generation. In *IEEE/CVF Conference on Computer Vision and Pattern Recognition (CVPR)*.
- Jamie Wynn and Daniyar Turmukhambetov. 2023. DiffusioNeRF: Regularizing Neural Radiance Fields with Denoising Diffusion Models. In *CVPR*.
- Jianfeng Xiang, Zelong Lv, Sicheng Xu, Yu Deng, Ruicheng Wang, Bowen Zhang, Dong Chen, Xin Tong, and Jialong Yang. 2024. Structured 3D Latents for Scalable and Versatile 3D Generation. arXiv preprint arXiv:2412.01506 (2024).
- Zhiwen Yan, Weng Fei Low, Yu Chen, and Gim Hee Lee. 2024. Multi-Scale 3D Gaussian Splatting for Anti-Aliased Rendering. In *2024 IEEE/CVF Conference on Computer Vision and Pattern Recognition (CVPR)*. IEEE Computer Society, Los Alamitos, CA, USA, 20923–20931. <https://doi.org/10.1109/CVPR52733.2024.01977>
- Lihe Yang, Bingyi Kang, Zilong Huang, Xiaogang Xu, Jiashi Feng, and Hengshuang Zhao. 2024a. Depth Anything: Unleashing the Power of Large-Scale Unlabeled Data. In *CVPR*.
- Lihe Yang, Bingyi Kang, Zilong Huang, Zhen Zhao, Xiaogang Xu, Jiashi Feng, and Hengshuang Zhao. 2024b. Depth Anything V2. arXiv:2406.09414 (2024).
- Chongjie Ye, Lingteng Qiu, Xiaodong Gu, Qi Zuo, Yushuang Wu, Zilong Dong, Liefeng Bo, Yuliang Xiu, and Xiaoguang Han. 2024. StableNormal: Reducing Diffusion Variance for Stable and Sharp Normal. *ACM Transactions on Graphics (TOG)* (2024).
- Alex Yu, Vickie Ye, Matthew Tancik, and Angjoo Kanazawa. 2021. pixelNeRF: Neural Radiance Fields from One or Few Images. In *CVPR*.
- Fanghua Yu, Jinjin Gu, Zheyuan Li, Jinfan Hu, Xiangtao Kong, Xintao Wang, Jingwen He, Yu Qiao, and Chao Dong. 2024b. Scaling Up to Excellence: Practicing Model Scaling for Photo-Realistic Image Restoration in the Wild. In *Proceedings of the IEEE/CVF Conference on Computer Vision and Pattern Recognition (CVPR)*.
- Wangbo Yu, Jinbo Xing, Li Yuan, Wenbo Hu, Xiaoyu Li, Zhipeng Huang, Xiangjun Gao, Tien-Tsin Wong, Ying Shan, and Yonghong Tian. 2024c. ViewCrafter: Taming Video Diffusion Models for High-fidelity Novel View Synthesis. arXiv preprint arXiv:2409.02048 (2024).
- Zehao Yu, Anpei Chen, Binbin Huang, Torsten Sattler, and Andreas Geiger. 2024a. Mip-Splatting: Alias-free 3D Gaussian Splatting. *Conference on Computer Vision and Pattern Recognition (CVPR)* (2024).
- Jiani Zeng, Honghao Deng, Yunyi Zhu, Michael Wessely, Axel Kilian, and Stefanie Mueller. 2021. Lenticular Objects: 3D Printed Objects with Lenticular Lens Surfaces That Can Change their Appearance Depending on the Viewpoint. In *The 34th Annual ACM Symposium on User Interface Software and Technology (Virtual Event, USA) (UIST '21)*. Association for Computing Machinery, New York, NY, USA, 1184–1196. <https://doi.org/10.1145/3472749.3474815>
- Zehao Zhu, Zhiwen Fan, Yifan Jiang, and Zhangyang Wang. 2023. FSGS: Real-Time Few-Shot View Synthesis using Gaussian Splatting. arXiv:2312.00451 [cs.CV]

	Input		Mesh	View1		View2		View3	
	Semantics	Views		Render	Normal	Render	Normal	Render	Normal
1	“Eagle” & “Falcon” & “Hawk”	[0,0] [0,90] [-90,0]							
2	“Cactus” & “Succulent” & “Bamboo”	[0,0] [0,90] [-90,0]							
3	“Great Wall” & “Shwedagon Pagoda” & “Big Ben”	[0,0] [0,130] [0,-130]							
4	“A Bulb Held by a Hand” & “A Person Wearing VR” & “A Human Sculpture”	[0,0] [0,130] [0,-130]							
5	“Fish” & “Fish” & “Shark”	[0,0] [0,120] [0,-120]							
6	“Girl” & “Magic Castle” & “Giant Snake”	Random Views							
7	“Fragile Egg” & “Soaring Chicken” & “Fallen Feather”	Random Views							

Fig. 7. **Gallery of Shape from Semantics.** We show the input to our method, the generated colored mesh, the rendering and normal results of each semantics. The textured meshes are rendered with Blender. The normal maps show that our generated shapes have meaningful geometries aligned with the renderings.

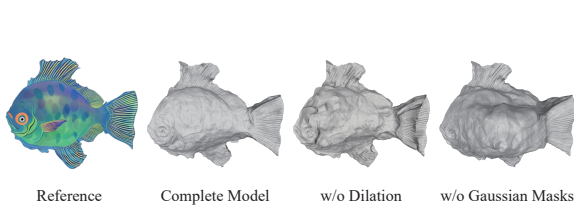


Fig. 8. **Ablation Study of Reconstruction Losses.** To make the geometric differences more obvious, the viewing angles of meshes are shifted slightly upwards compared to the reference image.

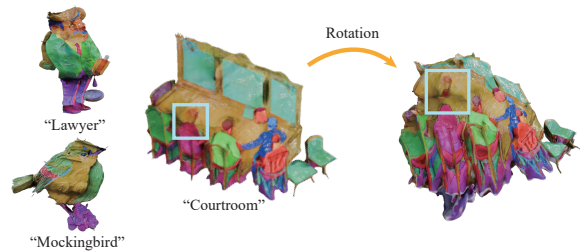


Fig. 9. **Limitations of Our Results.** Under specific semantics and views, while our generated results can achieve semantic alignment through visual misalignment, they lack geometric consistency.



Fig. 10. **Fabrication Results.** Results show that the manufactured outcomes are nearly identical to the simulations, delivering eye-catching visual effects.

Input		Wire Art	Ours
"Chair" & "Tiger"	[0,0]		
	[0,180]		
"Running Dog" & "Flying Bird"	[0,0]		
	[0,-90]		
"Old Man" & "Boat" & "Shark"	[0,0]		
	[0,120]		
	[-90,0]		
"Great Wall" & "Shwedagon Pagoda" & "Big Ben"	[0,0]		
	[0,130]		
	[0,-130]		

Fig. 11. **Comparison with Wire Art [Tojo et al. 2024].** We use the same semantics for comparison. The top-row result highlights the limitations of Wire Art, which arise from its dependence on projections to convey information. All results demonstrate that our model can capture perceptual 3D characteristics while delivering high levels of creativity, visual appeal.

Input	Shadow Art	Wire Art	Ours
"Eagle" & "Falcon" & "Hawk"			
"Cactus" & "Succulent" & "Bamboo"			

Fig. 12. **Comparison with Similar Works.** We compare with Shadow Art [Mitra and Pauly 2009], Wire Art [Tojo et al. 2024]. Considering that Shadow Art only accepts binary images as input, the inputs for Wire Art during comparison are RGB images restored in 3.2, while the inputs for Shadow Art are their masks. The input views are [0,0], [0,90], [-90,0]. The results illustrate that our models effectively integrate multiple semantic elements, presenting the information in a manner that is more readily perceivable to observers.